


## PAPER

[View Article Online](#)  
[View Journal](#) | [View Issue](#)Cite this: *Nanoscale Adv.*, 2022, 4, 77**Boron nitride nanotubes enhance mechanical properties of fibers from nanotube/polyvinyl alcohol dispersions†**Joe F. Khoury,  Jacob C. Vitale, Tanner L. Larson and Geyou Ao \*

Effectively translating the promising properties of boron nitride nanotubes (BNNTs) into macroscopic assemblies has vast potential for applications, such as thermal management materials and protective fabrics against hazardous environment. We spun fibers from aqueous dispersions of BNNTs in polyvinyl alcohol (PVA) solutions by a wet spinning method. Our results demonstrate that BNNTs/PVA fibers exhibit enhanced mechanical properties, which are affected by the nanotube and PVA concentrations, and the coagulation solvent utilized. Compared to the neat PVA fibers, we obtained roughly 4.3-, 12.7-, and 1.5-fold increases in the tensile strength, Young's modulus, and toughness, respectively, for the highest performing BNNTs/PVA fibers produced from dispersions containing as low as 0.1 mass% of nanotube concentration. Among the coagulation solvents tested, we found that solvents with higher polarity such as methanol and ethanol generally produced fibers with improved mechanical properties, where the fiber toughness shows a strong correlation with solvent polarity. These findings provide insights into assembling BNNTs-based fibers with improved mechanical properties for developing unique applications.

Received 8th September 2021  
Accepted 28th October 2021

DOI: 10.1039/d1na00677k

[rsc.li/nanoscale-advances](http://rsc.li/nanoscale-advances)**Introduction**

Macroscopic assembly of nanomaterials is a necessary route to achieve films and fibers with tunable properties for applications ranging from effective thermal management to multifunctional textiles. Liquid phase processing enables versatile nanomaterial assembly through providing access for the surface functionalization and integration with other nanomaterials and polymers for the overall property control and enhancement. Boron nitride nanotubes (BNNTs) have a hexagonal lattice structure similar to that of carbon nanotubes (CNTs) with alternating boron and nitrogen atoms.<sup>1</sup> BNNTs are lightweight and electrically insulating with a uniform wide band gap ( $\approx 6$  eV),<sup>2,3</sup> and have promising optical<sup>4</sup> and mechanical<sup>5</sup> properties, excellent thermal conductivity ( $350\text{--}2400$  W mK<sup>-1</sup>),<sup>6,7</sup> and high stability up to 900 °C in air.<sup>8</sup> This unique combination of material properties is ideal for applications, such as transparent protective coatings, thermal management in electronics and textiles, and biomedical applications.<sup>9–13</sup>

Effective translation of individual nanotube properties into BNNTs-based assemblies often requires tailoring interfaces through surface modification and uniformly dispersing

nanotubes in various solvents and polymer matrices. Non-covalent complexation of BNNTs with polymers, surfactants, and biomolecules through adsorption onto the surface of nanotubes is a simple and effective way of producing liquid dispersions of BNNTs.<sup>14–16</sup> This approach preserves the intrinsic properties of nanotubes as compared to the covalent functionalization of tubes, which often causes permanent changes in the B–N lattice structure and subsequent property deterioration.<sup>17–19</sup> In recent work, dispersions of BNNTs in solvents, including dimethyl formamide (DMF) and ethanol, have been integrated with polymer matrices to produce composites and fibers.<sup>12,20–22</sup> Particularly, significant improvement in thermal conductivity was obtained for BNNT-based composites prepared by vacuum filtration of aqueous dispersions of nanotube/polymer mixtures.<sup>22–24</sup> However, fiber spinning and mechanical property enhancement of BNNT assemblies remain to be challenging.

In comparison, multifunctional strong fibers from liquid dispersions of CNTs<sup>25–29</sup> and boron nitride nanosheets (BNNs),<sup>30</sup> that are one-dimensional (1D) and 2D counterparts of BNNTs, have been produced successfully *via* liquid-phase processing. During the past decades, CNTs have been combined with polymers, including polyvinyl alcohol (PVA) and polyacrylonitrile (PAN) that have been utilized for spinning industry scale fibers, to obtain composite fibers with significantly improved mechanical properties.<sup>26,28,31</sup> Particularly, Kumar and colleagues reported mechanical property improvements for CNTs/PAN fibers, including increases in modulus,

Department of Chemical and Biomedical Engineering, Washkewicz College of Engineering, Cleveland State University, 2121 Euclid Avenue, Cleveland, OH 44115, USA. E-mail: [g.ao@csuohio.edu](mailto:g.ao@csuohio.edu)

† Electronic supplementary information (ESI) available: Tables S1–S5 and Fig. S1–S9. See DOI: 10.1039/d1na00677k



tensile strength, and toughness by 75%, 70%, and 230%, respectively, in comparison to the neat PAN fibers.<sup>26</sup> However, BNNTs/PAN fibers produced recently by the same group exhibited diminished mechanical properties.<sup>12</sup> This is likely due to the poor dispersion of BNNTs and voids formed in fibers that are caused by impurities in the synthetic material, such as elemental boron, boron oxide ( $B_2O_3$ ), and hexagonal boron nitride (hBN) structures such as nanosheets and nanocages.<sup>32</sup> Therefore, BNNT fillers with improved purity and dispersion quality are needed for polymeric fiber reinforcement.

Here, we demonstrate that BNNTs coated by a strong surfactant, sodium deoxycholate (SDC), remain stable in PVA solutions, and wet spinning of BNNTs/PVA dispersions can produce fibers with significantly improved mechanical properties at a nanotube concentration of as low as 0.1 mass%. Specifically, we investigated the stabilization of BNNTs in water using various dispersing agents including surfactants, lysozyme (LSZ), and an LSZ/surfactant mixture. Among the dispersants tested, SDC stabilizes the largest amount of BNNTs in water and the resulting SDC-coated BNNTs (SDC-BNNTs) are highly stable when mixed with a PVA solution. Subsequently, we produced wet-spun fibers by injecting BNNTs/PVA mixtures in a rotating coagulation bath of methanol, ethanol, and a methanol/acetone mixture, respectively. Fibers were dried under ambient conditions before testing their mechanical properties. Various parameters including pristine *versus* purified BNNT material, BNNT and PVA concentrations, and the coagulation solvent were tested to study their effects on the overall mechanical properties, including tensile strength, Young's modulus, and toughness, of the final composite fibers.

## Experimental section

### Materials

Synthetic pristine (puffball, lot no: 426191,  $\approx 50$  mass% residual elemental boron impurity) and purified (refined puffball, lot no: CNA191011,  $<1$  mass% elemental boron) few-wall BNNT materials (*i.e.*, mostly 2–5 walls)<sup>16,33,34</sup> were purchased from BNNT, LLC (Newport News, VA). Sodium deoxycholate (SDC,  $\geq 98\%$  BioXtra), sodium dodecyl sulfate (SDS,  $\geq 99\%$  BioXtra), tetradecyl trimethylammonium bromide (TTAB,  $\geq 98\%$ ), lysozyme (LSZ) from chicken egg white (lyophilized powder, protein  $\geq 90\%$ ), and polyvinyl alcohol (PVA,  $M_w$  146 000–186 000) were obtained from Sigma-Aldrich. Ethanol (EtOH, 100%, Decon Labs, Inc.), methanol (MeOH, 99.9%, Alfa Aesar), and acetone (99.5+%, Alfa Aesar) were used as received.

### Nanotube sample preparation

For the study of dispersing agent selection, pristine BNNTs were dispersed in a total volume of 1 mL deionized (DI) water at  $1 \text{ mg mL}^{-1}$  (*i.e.*, 0.1 mass%) of the BNNT synthetic material using different dispersants. For SDC, SDS, and TTAB, the concentration of surfactant was kept at 1 mass%. In addition, a final concentration of  $10 \text{ mg mL}^{-1}$  (*i.e.*, 1 mass%) LSZ and a mixture of 0.5 mass% TTAB –  $5 \text{ mg mL}^{-1}$  (*i.e.*, 0.5 mass%) LSZ were used for dispersing BNNTs, respectively. For fiber spinning, both

pristine and purified BNNTs were dispersed at  $4 \text{ mg mL}^{-1}$  (*i.e.*, 0.4 mass%) of the BNNT synthetic material, respectively, in a total volume of 1 mL DI water using 1 mass% SDC. The mixture of BNNTs and a dispersing agent in water were bath sonicated for 30 min at room temperature, followed by probe tip ultrasonication (model VCX 130, Sonics and Materials, Inc.) in an ice bath at a power level of 8 W for 1 hour using a 2 mm diameter probe. Supernatant dispersions were collected after centrifugation at 2500g for 30 min at  $19^\circ\text{C}$  and were used as the stock BNNT dispersions.

### Dispersion characterization

UV-vis absorbance measurements were performed using a Jasco V-760 spectrophotometer over the wavelength range of 187–800 nm using a 10 mm path length quartz cuvette. Membrane filtration using a Microcon® centrifugal filter with a molecular weight cutoff (MWCO) of 100 kDa was performed to remove unbound, excess dispersants to allow resolution of nanotube absorption feature near 204 nm wavelength. For the measurements shown in Fig. 1, supernatant samples were membrane filtered three times and re-dispersed in water. The concentration of individually dispersed SDC-BNNT complexes was determined using an extinction coefficient of  $188.27 \text{ mL mg}^{-1} \text{ cm}^{-1}$  at 204 nm wavelength that is obtained in this work. Zeta potential measurements were obtained at room temperature for purified BNNTs stabilized by surfactants using a Malvern Zetasizer Nanoseries Nano-ZS with the dispersions injected into a folded capillary zeta cell. The excess, unbound surfactants were removed by membrane filtration as described previously.

### Fiber spinning of BNNTs and PVA mixtures

A stock solution of 10 mass% PVA was prepared by dissolving PVA crystalline powder in DI water under constant stirring for 3 hours at  $60^\circ\text{C}$  using a magnetic stir bar. The PVA stock was mixed with SDC-BNNT supernatant sample to obtain a total volume of 1 mL mixtures with final concentrations of 0–0.1 mass% BNNTs in 2.5 and 5 mass% PVA solutions, respectively. The BNNTs/PVA mixtures were gently vortexed for 1 min and bath sonicated for 30 min before fiber spinning. Specifically, a BNNTs/PVA mixture was injected at a flow rate of  $100 \mu\text{L min}^{-1}$  through a high-pressure 22 gauge (0.5 mm inner diameter) stainless steel needle using a syringe pump into a 400 mL coagulation bath (*i.e.*, MeOH, EtOH, and a cosolvent of MeOH/acetone containing 25 vol% acetone) rotating at 23 rpm. The needle is positioned 5 cm from the coagulation bath center. Fibers were pulled from the bath at an average rate of  $10 \text{ cm min}^{-1}$  and dried in air for at least 15 min before mechanical testing.

### Mechanical testing

An Instron Premium 5969 with a 5 N static load cell was used to test the mechanical properties of BNNTs/PVA fibers at an extension speed of  $1 \text{ mm min}^{-1}$ . Fiber samples were glued into a testing frame with a gauge length of 26 mm, which was then installed on pneumatic side-action grips of 50 N capacity with



smooth jaw faces (25 mm × 25 mm). The load and gauge length were balanced and zeroed before each run. Test data collected for each sample were load, extension, time, and strain. The densities of fibers were estimated to be 1.30 g cm<sup>-3</sup> for neat PVA fibers<sup>35,36</sup> and 1.28 g cm<sup>-3</sup> for BNNTs/PVA fibers using the rule of mixture where the density of BNNTs is 1.50 g cm<sup>-3</sup> by taking the average of previously reported values,<sup>37,38</sup> while densities for SDC and PVA are 1.01 and 1.30 g cm<sup>-3</sup>, respectively.<sup>35,36</sup> Excel and MATLAB were used to analyze the mechanical properties of fiber samples. Five different fiber samples were measured for each composition of BNNTs/PVA fibers. Of the five samples, the ones with the highest and lowest tensile strength were eliminated, and the remaining three samples were used to calculate the average mechanical properties of fibers.

### Scanning electron microscopy (SEM)

High-resolution field emission scanning electron microscope (SEM), Inspect F50 by FEI, equipped with an Everhart-Thornley detector with variable grid bias and electron dispersive spectroscopy (EDS) detector was used to image the surface and cross-section of fibers and perform elemental mapping of the fiber cross-section. After obtaining the cross-section area at fiber failure, the change in cross-section area with increasing elongation at a given time was determined using the equation,

$$A_t = (l_f \times A_f) / l_t,$$

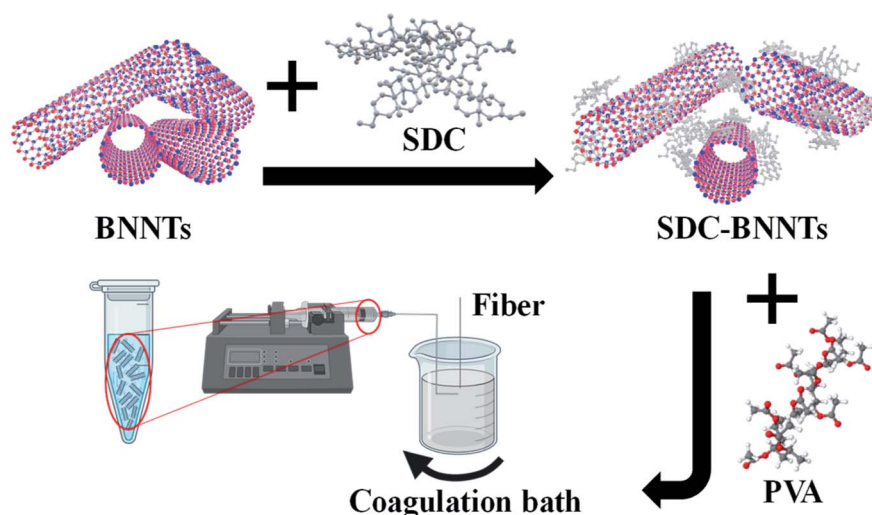
where,  $A_t$  is the cross-section area at time  $t$ ,  $A_f$  is the cross-section area at fiber failure,  $l_t$  is the fiber length at time  $t$ , and  $l_f$  is the fiber length at failure.

## Results and discussion

During the past decades, nanofillers have been used in polymer matrices to obtain strong composite fibers with multifunctional properties. PVA polymer has been widely utilized for commercial fibers in many applications due to its chemical and

mechanical stability.<sup>39</sup> Additionally, PVA is known to interact strongly with CNTs and BNNTs and causes the coagulation of nanomaterial dispersions to form composite fibers.<sup>40,41</sup> Particularly, PVA chains adsorb onto the surface of nanotubes causing bridging coagulation that significantly improves mechanical properties.<sup>28,41</sup> However, the interfacial interaction between PVA and CNTs may also lead to nanotube aggregations by displacing weak surface coatings of tubes, which limits versatile fiber spinning. Various dispersants including surfactants, such as SDS, TTAB and polyoxoethylene glycol octadecyl ether (*i.e.*, Brij® 78), and biomolecule LSZ have been utilized to successfully stabilize CNTs against aggregation in water when mixed with PVA.<sup>28,42</sup> Stable dispersions of BNNTs in water using surfactants with varying properties (*i.e.*, ionic and nonionic) have also been achieved previously.<sup>16</sup> In addition, PVA is shown to effectively disperse 2D BNNTs through hydrogen bonding interactions between the hydroxyl group of the polymer and the partially ionic B–N lattice structure due to an electron deficiency of B atoms.<sup>30,43</sup> Based on these previously known stabilization approaches of CNTs and BNNTs in PVA solutions, we fabricated BNNTs/PVA composite fibers by wet spinning, where nanotubes were initially dispersed in water using a strong surfactant SDC (Scheme 1).

We tested four dispersing agents including SDC, SDS, TTAB, LSZ, and a combination of TTAB/LSZ to compare their effectiveness in suspending the most BNNTs in water. SDC is an anionic surfactant known to interact with CNTs much stronger than other surfactants through forming a homogenous, bound interfacial layer of surfactants around tubes due to its rigid, steroid-ring structure.<sup>44,45</sup> The SDC–nanotube complexes are subsequently stabilized in water *via* electrostatic interactions. Here, the supernatant dispersions of BNNTs coated by various dispersants showed the characteristic BNNT absorption peak at 204 nm wavelength (Fig. 1a). Particularly, supernatants were collected after centrifugation at 2500g, which was found to be optimal in retaining the largest amount of dispersed BNNTs in water while removing most nanotube bundles and impurities



Scheme 1 BNNTs/PVA fiber spinning process.



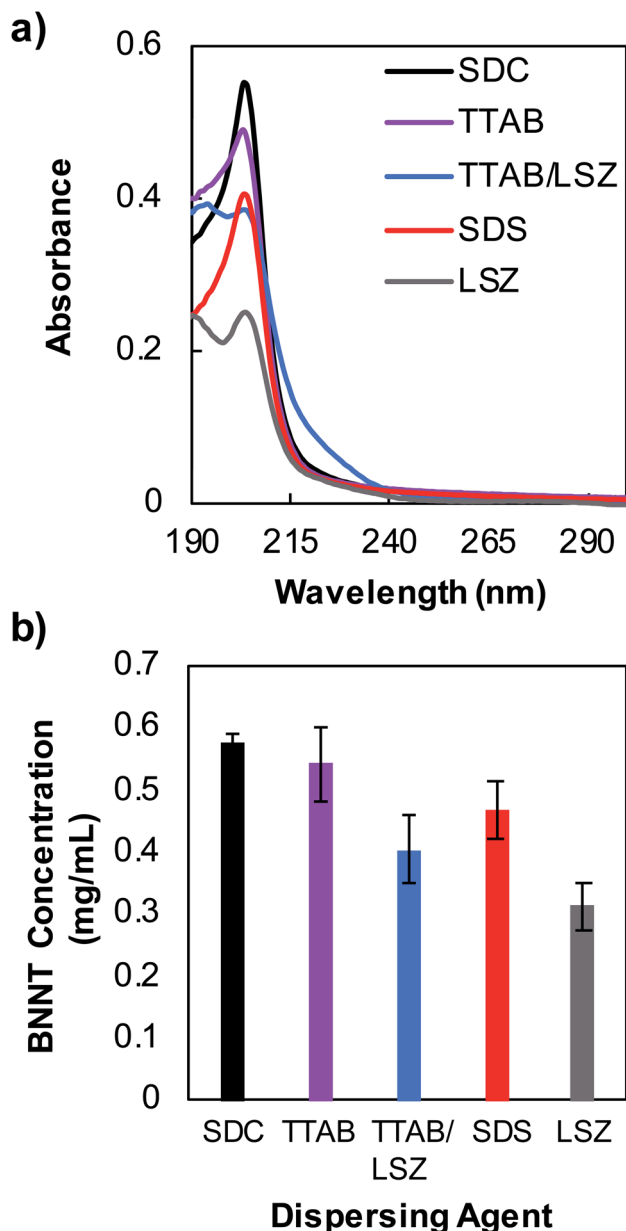


Fig. 1 Dispersions of pristine BNNTs in water stabilized by various dispersing agents including SDC, TTAB, TTAB/LSZ, SDS, and LSZ. (a) Absorbance spectra of supernatant dispersions of BNNTs and the corresponding (b) concentration of dispersed BNNT complexes. All samples were diluted by a factor of 200 $\times$  in DI water for UV-vis absorbance measurements. The error bars were obtained from the standard deviation of a minimum of three repeats of different dispersion samples.

(Fig. S1†). This is evidenced by a well-resolved, narrower absorption peak and diminished baseline absorbance for supernatant dispersions compared to that of a bulk dispersion without centrifugation (Fig. S1a†). Additionally, among the dispersants tested at the experimental condition in this work, SDC stabilizes the most tubes in supernatants (*i.e.*,  $\approx 0.57$  mg mL<sup>-1</sup> of SDC-BNNTs) based on an extinction coefficient of 188.27 mL mg<sup>-1</sup> cm<sup>-1</sup> at 204 nm obtained for SDC-BNNTs

(Fig. 1b and S2†). The stock dispersions of SDC-BNNTs obtained in this work are stable for weeks for a routine storage condition at 4 °C. The concentration of nanotubes in supernatant samples is followed by BNNTs dispersed by a cationic surfactant TTAB, anionic SDS, a mixture of TTAB and cationic LSZ, and LSZ alone. In Fig. 1b, the slightly higher BNNT concentration obtained by cationic TTAB as compared to anionic SDS is likely due to the increased interaction between the cationic surfactant and the BNNTs, which possess N atoms with partial negative charges.<sup>16</sup> The longer aliphatic chain of TTAB (*i.e.*, 14-carbon tail) may further increase the hydrophobic interaction with BNNTs than SDS, which has a slightly shorter chain length of 12 carbons. The magnitude of zeta potentials of surfactant-coated BNNTs is found to be similar (*i.e.*, -53, -57, and +52 mV for SDC-, SDS, and TTAB-dispersed BNNTs), indicating stable dispersions of nanotubes due to electrostatic stabilization in water (Table S1†). However, the absence of steroid-ring structure in TTAB and SDS may lead to the stabilization of a lesser amount of BNNTs in water compared to SDC. Additionally, we utilized LSZ, a globular protein of roughly 3 nm diameter, to test its capability to disperse BNNTs; however, it resulted in dispersions with the lowest nanotube concentration among all the dispersants tested in this work. LSZ is known to interact with single-wall carbon nanotubes (SWCNTs) of  $\approx 1$  nm diameter through  $\pi$ - $\pi$  stacking and hydrophobic interactions between tryptophan (aromatic amino acid residue) and the nanotube sidewall.<sup>46-48</sup> The specific structural motif and the rigidity of LSZ are also considered to play a role in its selective interaction with nanotubes of different diameters.<sup>46</sup> When interacting with BNNTs of larger diameter (*i.e.*, roughly 7 nm),<sup>19,49</sup> the wrapping of nanotubes by LSZ may have been hindered. Adding TTAB in LSZ solution increases the BNNT concentration in dispersions. This is similar to the dispersion outcome of SWCNTs stabilized by a mixture of TTAB/LSZ, where the improved dispersion stability of nanotubes is likely caused by the synergistic interaction of TTAB and the amino acid residues of LSZ as well as interaction of TTAB/LSZ complexes with nanotubes.<sup>50</sup> Complex interactions and stability of BNNT dispersions in proteins and mixtures of protein/surfactant are worthy of future studies, particularly for developing BNNT complexes with improved biocompatibility and functionality for biomedical applications. Here, we selected SDC-BNNT complexes due to its ability to disperse the most BNNTs and remain stable when combined with PVA in water for fabricating BNNTs/PVA fibers by wet spinning.

Wet spinning of fibers has been applied conventionally in many industries due to its robustness, scalability, cost effectiveness, and accessibility for process and material optimization. We studied the effects of various processing conditions on the overall mechanical properties of wet-spun BNNTs/PVA fibers by combining SDC-BNNT dispersions with aqueous solutions of PVA and fabricated fibers in coflowing streams of a coagulation solvent. The nanotube length, together with aspect ratio and purity, is known to impact fiber mechanical properties where longer tubes lead to greater strength due to an improved tube-tube stress transfer.<sup>25,51</sup> We estimate the number average length of SDC-BNNTs to be roughly 324  $\pm$





133 nm based on our prior work utilizing the same sample dispersion method.<sup>52</sup> To begin with, we tested how the purity of BNNT synthetic material, and the nanotube concentration affect the mechanical properties of fibers coagulated in EtOH, while keeping the PVA content in BNNTs/PVA dispersions at 5 mass% (Fig. 2, Tables S2 and S3†). We estimated the volume fractions of BNNTs (*i.e.*, roughly from 0.5 to 1.6 vol% BNNTs) in dried BNNTs/PVA fibers based on the compositions of BNNTs/PVA dispersions (Table S2†). Typical stress-strain curves of fibers produced from mixtures of BNNTs/PVA using pristine and purified BNNTs are shown in Fig. S3 and S4.† In general, the overall mechanical properties of BNNTs/PVA fibers show significant improvement over neat PVA fibers with increasing nanotube concentration.

Specifically, the average tensile strength of fibers increases monotonically with BNNT concentration, where the addition of as low as 0.025 mass% of purified BNNTs in the dispersion results in an increased tensile strength for purified BNNTs/PVA fibers to  $\approx 307 \pm 62$  MPa, which is roughly 66% higher than that of neat PVA fibers (Fig. 2a). With further increase in the concentration of purified BNNTs up to 0.1 mass%, the fiber tensile strength increases to  $553 \pm 45$  MPa, corresponding to a 3.0-fold increase than that of neat PVA fibers (*i.e.*,  $185 \pm 45$

MPa). In comparison, the average Young's modulus of purified BNNTs/PVA fibers increases at 0.025 mass% BNNTs to  $3.8 \pm 0.5$  GPa, which remains relatively the same at 0.05 mass% of nanotubes (Fig. 2b). This is followed by a sharp increase at 0.075 mass% of purified BNNTs to  $7.1 \pm 1.0$  GPa, which is 6.4-fold higher than that of the neat PVA fibers (*i.e.*,  $1.1 \pm 0.1$  GPa). The Young's modulus of purified BNNTs/PVA fibers remains unchanged when nanotube concentration is increased to 0.1 mass%. Utilizing the rule of mixture,<sup>53,54</sup> we estimated the effective modulus of purified BNNTs in BNNTs/PVA fibers, which are higher than that of pristine BNNTs, to be from  $289 \pm 4$  to  $620 \pm 75$  GPa depending on the BNNT content in the fibers (Fig. S5†). These are within 24–52% range of the Young's modulus of an individual BNNTs (*i.e.*,  $\approx 1.2$  TPa).<sup>5</sup> The average toughness of purified BNNTs/PVA fibers increases gradually as a function of nanotube concentration to  $166 \pm 55$  J g<sup>-1</sup> at 0.1 mass% BNNTs, which is 48% higher than that of neat PVA fibers (*i.e.*,  $112 \pm 32$  J g<sup>-1</sup>) (Fig. 2c). Additionally, fibers containing purified BNNTs with <1 mass% elemental boron impurities show slightly improved mechanical properties than those produced from dispersions of pristine BNNTs ( $\approx 50\%$  elemental boron) within the nanotube concentration range that we have tested in this work. This indicates that at a lower loading of

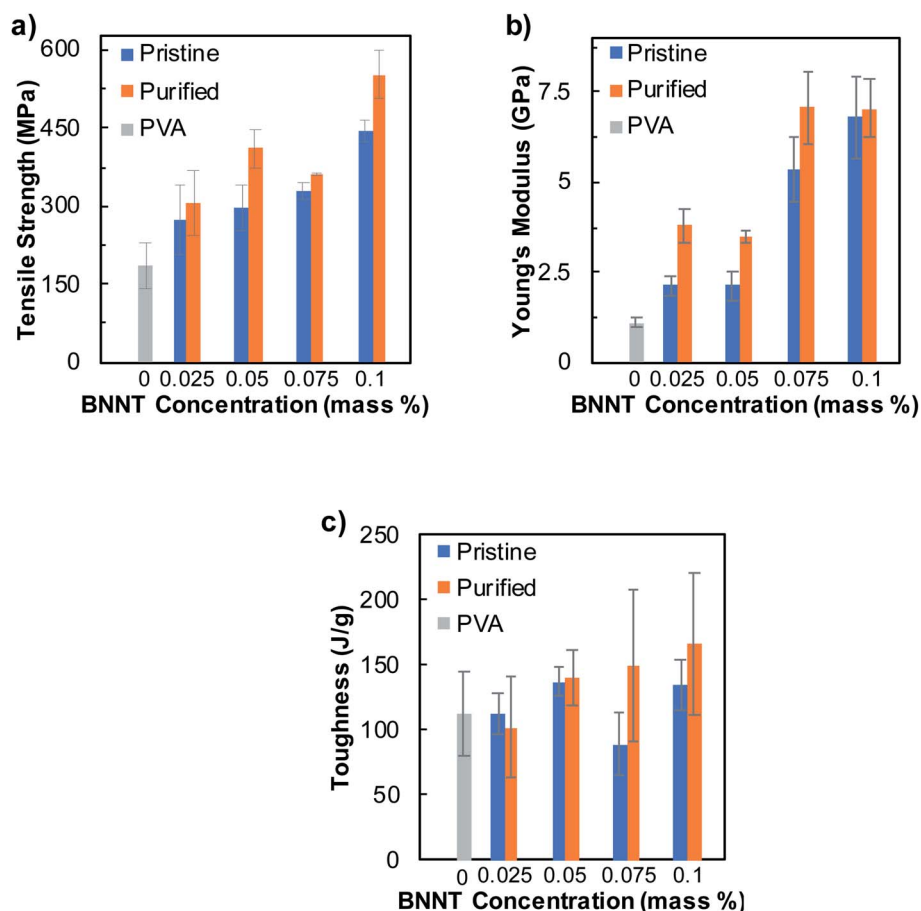


Fig. 2 Mechanical properties including (a) tensile strength, (b) Young's modulus, and (c) toughness of neat PVA (*i.e.*, PVA), pristine BNNTs/PVA (*i.e.*, pristine), and purified BNNTs/PVA (*i.e.*, purified) fibers produced from dispersions containing 5 mass% PVA and varying BNNT concentrations in an EtOH coagulation bath.



BNNT material (*i.e.*, less than 0.1 mass% tubes), the elemental boron impurity may have a minor impact on the overall mechanical properties of BNNTs/PVA fibers. Further purification of BNNT material by removing non-nanotube hBN structures such as nanosheets and nanocages in future work could be beneficial for improving mechanical properties of BNNTs-based fibers. Additionally, evaluating the effect of BNNTs on the overall property of BNNTs/polymer fibers at a broad concentration range and further modifying the fiber spinning process are worthy of future studies.

The fiber surface morphology and the inner fiber structures are inspected using SEM (Fig. 3, S6 and S7†). The flexibility and mechanical robustness of BNNTs/PVA fibers spun in EtOH are demonstrated by tying a fiber into a knot without breaking (Fig. 3a). Representative SEM images show the smooth surface morphology of fibers and assist the determination of fiber cross-section areas. Generally, the average cross-section area of fibers decreases with increasing nanotube concentration from  $539 \pm 245 \mu\text{m}^2$  for neat PVA fibers to  $147 \pm 67 \mu\text{m}^2$  for BNNTs/PVA fibers containing 0.1 mass% tubes. With increasing nanotube concentration in BNNTs/PVA dispersions, samples became visibly more viscous, which likely led to the difference in the cross-section area of fibers under applied shear during the spinning process. The inner structures differ between BNNTs/PVA fibers containing pristine and purified nanotubes as well. BNNTs/PVA fibers composed of pristine nanotubes that are coagulated in EtOH show microvoids throughout the fiber cross-section, likely due to impurities such as elemental boron and hBN nanostructures (Fig. 3b and c). Regardless of the seemingly porous structure, fibers containing pristine BNNTs demonstrate better mechanical properties than neat PVA fibers. In comparison, BNNTs/PVA fibers containing purified nanotubes exhibit a cross-section of relatively smooth structure (Fig. 3d). This indicates that purified BNNT sample may integrate well with PVA aqueous solution, resulting in BNNTs/PVA fibers with more uniform structures and higher overall mechanical properties than fibers containing pristine tubes.

We then tested additional parameters including PVA concentration and the type of coagulation solvent used in the fiber spinning process and investigated their effects on the fiber mechanical properties. First, we reduced the PVA concentration from 5 mass% to 2.5 mass% in pristine BNNTs/PVA mixtures, while keeping the concentration of pristine BNNTs at 0.1 mass%, and spun fibers in EtOH (Fig. 4, S8, and Table S4†). Stronger fibers were obtained from BNNTs/PVA mixtures containing 2.5 mass% PVA including a tensile strength of  $757 \pm 147 \text{ MPa}$  and a Young's modulus of  $14.0 \pm 3.4 \text{ GPa}$ , which are 1.7- and 2.1-folds higher than those of fibers containing 5 mass% PVA, respectively (Fig. 4a and Table S4†). Moreover, these values correspond to 4.1- and 12.7-fold increases of tensile strength and Young's modulus values than that of neat PVA fibers obtained from 5 mass% PVA in EtOH (Table S3†). Nanotube orientation plays an important role in fiber overall properties, including modulus.<sup>25,51</sup> Reducing PVA concentration in BNNTs/PVA mixtures likely results in decreased viscosity of dispersions favoring improved nanotube orientation during extrusion from a needle, and the nanotube orientation is further assisted by the coflowing streams of EtOH bath. This likely results in enhanced strength and stiffness of fibers produced from BNNTs/PVA mixtures with 2.5 mass% PVA. However, the average toughness of fibers decreases by roughly 18% to  $111 \pm 30 \text{ J g}^{-1}$  for BNNTs/PVA fibers when PVA concentration in mixtures decreases from 5 to 2.5 mass% (Fig. 4b). This is related to the decreasing strain at break from  $69 \pm 13\%$  to  $60 \pm 23\%$  resulting from the reduced PVA content in BNNTs/PVA mixtures for fiber spinning. It is noteworthy to mention that coagulated fibers from 2.5 mass% PVA solution without adding BNNTs are too weak to be drawn from the EtOH bath. This indicates that BNNTs assist the formation of BNNTs/PVA fiber through reinforcing the PVA polymer matrix and improve the overall mechanical properties of BNNTs/PVA fibers synergistically.

Additionally, we performed a preliminary study to evaluate the effect of the coagulation solvent on the mechanical properties of fibers spun from pristine BNNTs/PVA mixtures

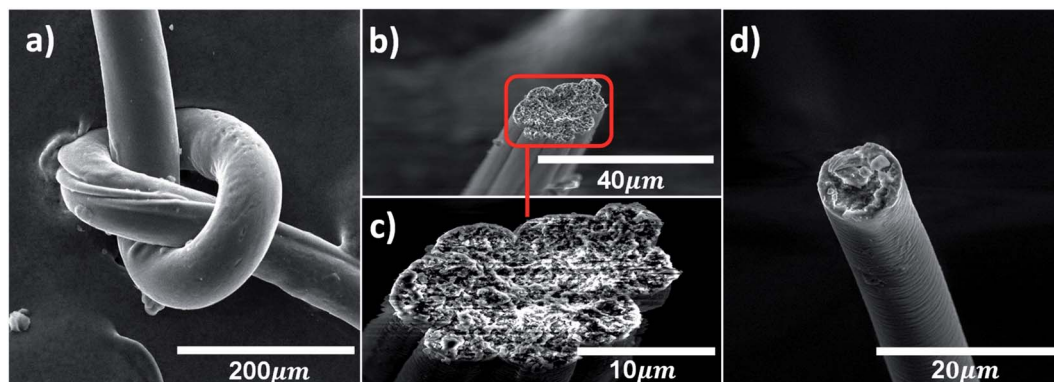


Fig. 3 SEM images of BNNTs/PVA fibers produced from dispersions containing 5 mass% PVA in an EtOH coagulation bath. (a) A fiber obtained from a dispersion of 0.1 mass% pristine BNNTs showing the mechanical robustness (knot). The scale bar is 200  $\mu\text{m}$ . The cross-section of fibers obtained from dispersions containing (b and c) 0.1 mass% pristine BNNTs and (d) 0.1 mass% purified BNNTs. The scale bars are 10, 20, and 40  $\mu\text{m}$ , respectively.



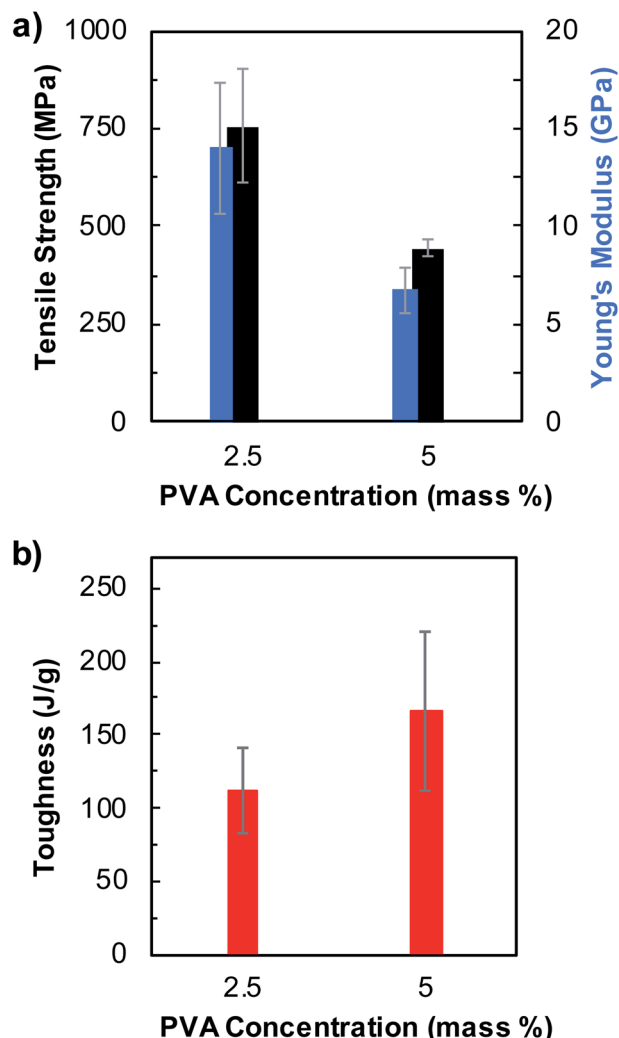


Fig. 4 Mechanical properties including (a) tensile strength, Young's modulus and (b) toughness of pristine BNNTs/PVA fibers produced from dispersions containing 0.1 mass% BNNTs and different PVA concentrations of 2.5 and 5 mass%, respectively, in an EtOH coagulation bath.

containing 0.1 mass% pristine BNNTs and 2.5 mass% PVA (Fig. 5, S9, and Table S5†). Solvents of varying polarity and dielectric constants including MeOH, EtOH, and a MeOH/acetone cosolvent containing 25 vol% acetone were utilized to coagulate BNNTs/PVA fibers. MeOH and EtOH are known to facilitate the coagulation of PVA fibers.<sup>30,55,56</sup> When acetone was utilized alone, neither PVA solution nor BNNTs/PVA dispersions were coagulated into fibers as the spinning solution form a ball of gel sticking to the needle. In general, BNNTs/PVA fibers coagulated in MeOH/acetone cosolvent show inferior mechanical properties than those in pure alcohol solvents. Between MeOH and EtOH, the average tensile strength of BNNTs/PVA fibers slightly increases to  $789 \pm 46$  MPa (*i.e.*, 4.3-fold higher than that of neat PVA fibers) when MeOH is used as the coagulation solvent (Fig. 5a and Table S5†). As for the Young's modulus, EtOH produces fibers with a higher value (*i.e.*,  $14.0 \pm 3.4$  GPa), which is  $\approx 44\%$  larger than those obtained in MeOH

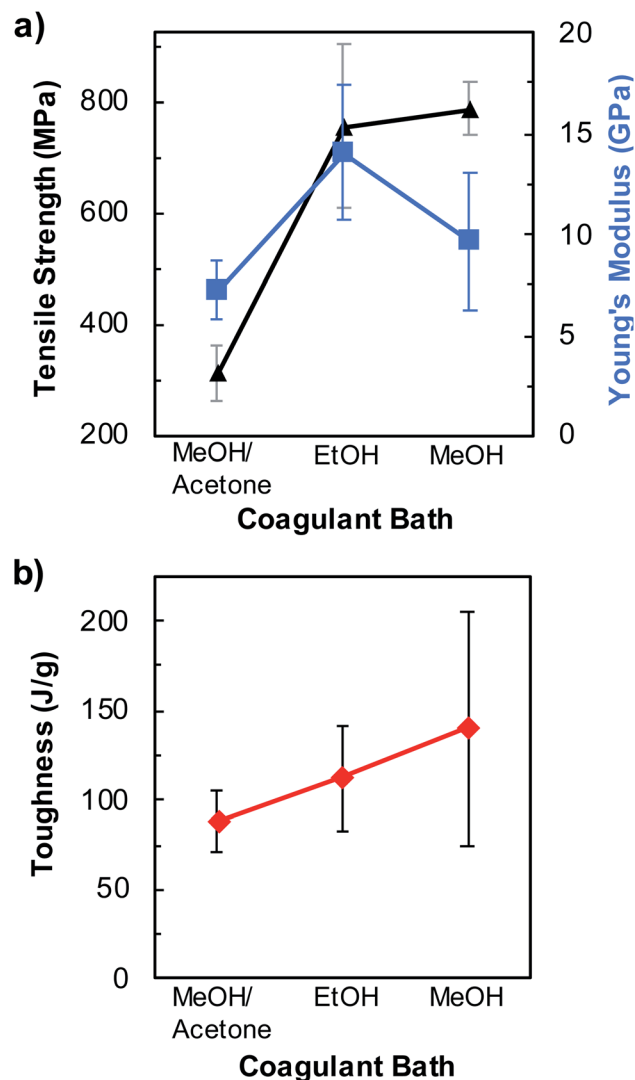


Fig. 5 Mechanical properties including (a) tensile strength, Young's modulus, and (b) toughness of pristine BNNTs/PVA fibers produced from dispersions containing 0.1 mass% BNNTs and 2.5 mass% PVA in different coagulation baths including MeOH, EtOH, and MeOH/acetone cosolvent of 25 vol% acetone.

(Fig. 5a and Table S5†). Additionally, the fiber toughness increases linearly with increasing solvent polarity reaching an average value of  $140 \pm 65$  J g<sup>-1</sup> for BNNTs/PVA fibers in MeOH (Fig. 5b). The effect of solvent properties on the mechanical properties of BNNTs/PVA fibers will be rationalized by future studies to facilitate the production of strong fibers with enhanced performance.

## Conclusion

In summary, we have demonstrated that effective dispersions of BNNTs lead to significantly improved mechanical properties of the resulting BNNTs/PVA fibers at a nanotube concentration of as low as 0.1 mass%. Particularly, surfactant-dispersed BNNTs are stable in PVA solution and BNNTs/PVA fibers can be produced by wet fiber spinning in various coagulation solvents



including MeOH, EtOH, and a MeOH/acetone mixture. At a constant concentration of 5 mass% PVA, tensile strength and Young's modulus of fibers produced in EtOH improve with increasing BNNT concentration that have been tested in this work. When decreasing the PVA concentration to 2.5 mass% in pristine BNNTs/PVA dispersions, the tensile strength and Young's Modulus of fibers spun in EtOH increase to  $757 \pm 147$  MPa and  $14.0 \pm 3.4$  GPa, respectively. This corresponds to 4.1- and 12.7-fold increases as compared to that of neat PVA fibers produced from 5 mass% PVA solution. A slightly higher tensile strength of  $789 \pm 46$  MPa (*i.e.*, 4.3-fold higher than that of neat PVA fibers) is obtained for pristine BNNTs/PVA fibers with MeOH as the coagulation solvent. The overall mechanical properties of fibers improve slightly with purified BNNTs than pristine BNNTs, suggesting that the elemental boron impurity has a minor effect on fiber properties within the BNNT loading range tested in this work. Separating nanotubes from non-nanotube hBN structures that are present in the synthetic material in future studies will better reveal the effect of impurities on fiber properties. In addition, further improvements in fiber processing, such as introducing controlled drawing and drying of fibers and optimizing fiber components and coagulation solvents, are planned in future work to achieve BNNTs-based fibers with enhanced performance. Combined, our work contributes to the potential macroscopic assembly of BNNTs, such as multifunctional, strong fibers for applications in thermal management and protective fabrics.

## Conflicts of interest

The authors declare no competing financial interest.

## Acknowledgements

We acknowledge the support of Cleveland State University (CSU) Faculty Start-Up Funds and Faculty Research Development Award. This work is partially supported by the National Science Foundation award (CMMI-2118416).

## References

- 1 D. Golberg, Y. Bando, Y. Huang, T. Terao, M. Mitome, C. Tang and C. Zhi, Boron Nitride Nanotubes and Nanosheets, *ACS Nano*, 2010, **4**, 2979–2993.
- 2 X. Blase, A. Rubio, S. G. Louie and M. L. Cohen, Stability and Band Gap Constancy of Boron Nitride Nanotubes, *EPL*, 1994, **28**, 335–340.
- 3 J. S. Lauret, R. Arenal, F. Ducastelle, A. Loiseau, M. Cau, B. Attal-Tretout, E. Rosencher and L. Goux-Capes, Optical Transitions in Single-Wall Boron Nitride Nanotubes, *Phys. Rev. Lett.*, 2005, **94**, 1–4.
- 4 P. Jaffrennou, J. Barjon, J. S. Lauret, A. Maguer, D. Golberg, B. Attal-Trétout, F. Ducastelle and A. Loiseau, Optical Properties of Multiwall Boron Nitride Nanotubes, *Phys. Status Solidi B*, 2007, **244**, 4147–4151.
- 5 R. Arenal, M.-S. Wang, Z. Xu, A. Loiseau and D. Golberg, Young Modulus, Mechanical and Electrical Properties of Isolated Individual and Bundled Single-Walled Boron Nitride Nanotubes, *Nanotechnology*, 2011, **22**, 265704.
- 6 C. W. Chang, A. M. Fennimore, A. Afanasiev, D. Okawa, T. Ikuno, H. Garcia, D. Li, A. Majumdar and A. Zettl, Isotope Effect on the Thermal Conductivity of Boron Nitride Nanotubes, *Phys. Rev. Lett.*, 2006, **97**, 085901.
- 7 B. E. Belkerk, A. Achour, D. Zhang, S. Sahli, M. A. Djouadi and Y. K. Yap, Thermal Conductivity of Vertically Aligned Boron Nitride Nanotubes, *Appl. Phys. Express*, 2016, **9**, 075002.
- 8 Y. Chen, J. Zou, S. J. Campbell and G. le Caer, Boron Nitride Nanotubes: Pronounced Resistance to Oxidation, *Appl. Phys. Lett.*, 2004, **84**, 2430–2432.
- 9 K. S. Kim, M. J. Kim, C. Park, C. C. Fay, S. H. Chu, C. T. Kingston and B. Simard, Scalable Manufacturing of Boron Nitride Nanotubes and Their Assemblies: A Review, *Semicond. Sci. Technol.*, 2017, **32**, 013003.
- 10 S. Pandit, K. Gaska, V. R. S. S. Mokkaapati, S. Forsberg, M. Svensson, R. Kádár and I. Mijakovic, Antibacterial Effect of Boron Nitride Flakes with Controlled Orientation in Polymer Composites, *RSC Adv.*, 2019, **9**, 33454–33459.
- 11 C. Zhang, R. Huang, Y. Wang, Z. Wu, H. Zhang, Y. Li, W. Wang, C. Huang and L. Li, Self-Assembled Boron Nitride Nanotube Reinforced Graphene Oxide Aerogels for Dielectric Nanocomposites with High Thermal Management Capability, *ACS Appl. Mater. Interfaces*, 2020, **12**, 1436–1443.
- 12 H. Chang, M. Lu, J. Luo, J. G. Park, R. Liang, C. Park and S. Kumar, Polyacrylonitrile/Boron Nitride Nanotubes Composite Precursor and Carbon Fibers, *Carbon*, 2019, **147**, 419–426.
- 13 M. B. Jakubinek, B. Ashrafi, Y. Martinez-Rubi, J. Guan, M. Rahmat, K. S. Kim, S. Dénommée, C. T. Kingston and B. Simard, Boron Nitride Nanotube Composites and Applications, *Nanotube Superfiber Mater.*, 2019, 91–111.
- 14 V. R. Kode, M. E. Thompson, C. McDonald, J. Weicherding, T. D. Dobrila, P. S. Fodor, C. L. Wirth and G. Ao, Purification and Assembly of DNA-Stabilized Boron Nitride Nanotubes into Aligned Films, *ACS Appl. Nano Mater.*, 2019, **2**, 2099–2105.
- 15 Z. J. Jakubek, M. Chen, Y. Martinez Rubi, B. Simard and S. Zou, Conformational Order in Aggregated Rra-P3HT as an Indicator of Quality of Boron Nitride Nanotubes, *J. Phys. Chem. Lett.*, 2020, **11**, 4179–4185.
- 16 A. D. Smith McWilliams, C. A. de Los Reyes, L. Liberman, S. Ergülen, Y. Talmon, M. Pasquali and A. A. Martí, Surfactant-Assisted Individualization and Dispersion of Boron Nitride Nanotubes, *Nanoscale Adv.*, 2019, **1**, 1096–1103.
- 17 C. Y. Zhi, Y. Bando, T. Terao, C. C. Tang, H. Kuwahara and D. Golberg, Chemically Activated Boron Nitride Nanotubes, *Chem.-Asian J.*, 2009, **4**, 1536–1540.
- 18 H. Shin, J. Guan, M. Z. Zgierski, K. S. Kim, C. T. Kingston and B. Simard, Covalent Functionalization of Boron Nitride Nanotubes via Reduction Chemistry, *ACS Nano*, 2015, **9**, 12573–12582.





- 19 C. A. de Los Reyes, K. L. Walz Mitra, A. D. Smith, S. Yazdi, A. Lored, F. J. Frankovsky, E. Ringe, M. Pasquali and A. A. Martí, Chemical Decoration of Boron Nitride Nanotubes Using the Billups-Birch Reaction: Toward Enhanced Thermostable Reinforced Polymer and Ceramic Nanocomposites, *ACS Appl. Nano Mater.*, 2018, **1**, 2421–2429.
- 20 T. M. Akintola, P. Tran, R. Downes Sweat and T. Dickens, Thermomechanical Multifunctionality in 3D-Printed Polystyrene-Boron Nitride Nanotubes (BNNT) Composites, *J. Compos. Sci.*, 2021, **5**, 61.
- 21 D. Kim, M. You, J. H. Seol, S. Ha and Y. A. Kim, Enhanced Thermal Conductivity of Individual Polymeric Nanofiber Incorporated with Boron Nitride Nanotubes, *J. Phys. Chem. C*, 2017, **121**, 7025–7029.
- 22 X. Zeng, J. Sun, Y. Yao, R. Sun, J. B. Xu and C. P. Wong, A Combination of Boron Nitride Nanotubes and Cellulose Nanofibers for the Preparation of a Nanocomposite with High Thermal Conductivity, *ACS Nano*, 2017, **11**, 5167–5178.
- 23 S. Quiles-Díaz, Y. Martínez-Rubí, J. Guan, K. S. Kim, M. Couillard, H. J. Salavagione, M. A. Gómez-Fatou and B. Simard, Enhanced Thermal Conductivity in Polymer Nanocomposites via Covalent Functionalization of Boron Nitride Nanotubes with Short Polyethylene Chains for Heat-Transfer Applications, *ACS Appl. Nano Mater.*, 2019, **2**, 440–451.
- 24 M. B. Jakubinek, J. F. Niven, M. B. Johnson, B. Ashrafi, K. S. Kim, B. Simard and M. A. White, Thermal Conductivity of Bulk Boron Nitride Nanotube Sheets and Their Epoxy-Impregnated Composites, *Phys. Status Solidi A*, 2016, **213**, 2237–2242.
- 25 N. Behabtu, C. C. Young, D. E. Tsentalovich, O. Kleinerman, X. Wang, A. W. K. Ma, E. A. Bengio, R. F. ter Waarbeek, J. J. de Jong, R. E. Hoogerwerf, S. B. Fairchild, J. B. Ferguson, B. Maruyama, J. Kono, Y. Talmon, Y. Cohen, M. J. Otto and M. Pasquali, Strong, Light, Multifunctional Fibers of Carbon Nanotubes with Ultrahigh Conductivity, *Science*, 2013, **339**, 182–186.
- 26 H. G. Chae, T. v. Sreekumar, T. Uchida and S. Kumar, A Comparison of Reinforcement Efficiency of Various Types of Carbon Nanotubes in Polyacrylonitrile Fiber, *Polymer*, 2005, **46**, 10925–10935.
- 27 D. W. Horn, G. Ao, M. Maugey, C. Zakri, P. Poulin and V. A. Davis, Dispersion State and Fiber Toughness: Antibacterial Lysozyme-Single Walled Carbon Nanotubes, *Adv. Funct. Mater.*, 2013, **23**, 6082–6090.
- 28 C. Mercader, V. Denis-Lutard, S. Jestin, M. Maugey, A. Derré, C. Zakri and P. Poulin, Scalable Process for the Spinning of PVA-Carbon Nanotube Composite Fibers, *J. Appl. Polym. Sci.*, 2012, **125**, E191–E196.
- 29 B. Vigolo, A. Penicaud, C. Coulon, C. Sauder, R. Paillet, C. Journet, P. Bernier and P. Poulin, Macroscopic Fibers and Ribbons of Oriented Carbon Nanotubes, *Science*, 2000, **290**, 1331–1334.
- 30 T. Gao, Z. Yang, C. Chen, Y. Li, K. Fu, J. Dai, E. M. Hitz, H. Xie, B. Liu, J. Song, B. Yang and L. Hu, Three-Dimensional Printed Thermal Regulation Textiles, *ACS Nano*, 2017, **11**, 11513–11520.
- 31 Y. Liu and S. Kumar, Polymer/Carbon Nanotube Nano Composite Fibers-A Review, *ACS Appl. Mater. Interfaces*, 2014, **6**, 6069–6087.
- 32 O. Kleinerman, M. Adnan, D. M. Marincel, A. W. K. Ma, E. A. Bengio, C. Park, S. H. Chu, M. Pasquali and Y. Talmon, Dissolution and Characterization of Boron Nitride Nanotubes in Superacid, *Langmuir*, 2017, **33**, 14340–14346.
- 33 M. W. Smith, K. C. Jordan, C. Park, J.-W. Kim, P. T. Lillehei, R. Crooks and J. S. Harrison, Very Long Single- and Few-Walled Boron Nitride Nanotubes via the Pressurized Vapor/Condenser Method, *Nanotechnology*, 2009, **20**, 505604.
- 34 O. Kleinerman, M. Adnan, D. M. Marincel, A. W. K. Ma, E. A. Bengio, C. Park, S.-H. Chu, M. Pasquali and Y. Talmon, Dissolution and Characterization of Boron Nitride Nanotubes in Superacid, *Langmuir*, 2017, **33**, 14340–14346.
- 35 B. Nematollahi, S. M. Asce, J. Sanjayan, F. Uddin and A. Shaikh, Tensile Strain Hardening Behavior of PVA Fiber-Reinforced Engineered Geopolymer Composite, *J. Mater. Civ. Eng.*, 2015, **27**, 04015001.
- 36 J. Luo, Q. Li, T. Zhao, S. Gao and S. Sun, Bonding and Toughness Properties of PVA Fibre Reinforced Aqueous Epoxy Resin Cement Repair Mortar, *Constr. Build. Mater.*, 2013, **49**, 766–771.
- 37 M. Mutz, E. Eastwood and M. D. Dadmun, Quantifying the Solubility of Boron Nitride Nanotubes and Sheets with Static Light Scattering and Refractometry, *J. Phys. Chem. C*, 2013, **117**, 13230–13238.
- 38 C. Zhi, Y. Bando, C. Tang and D. Golberg, Specific Heat Capacity and Density of Multi-Walled Boron Nitride Nanotubes by Chemical Vapor Deposition, *Solid State Commun.*, 2011, **151**, 183–186.
- 39 M. Aslam, M. A. Kalyar and Z. A. Raza, Polyvinyl Alcohol: A Review of Research Status and Use of Polyvinyl Alcohol Based Nanocomposites, *Polym. Eng. Sci.*, 2018, 2119–2132.
- 40 P. Poulin, B. Vigolo and P. Launois, Films and Fibers of Oriented Single Wall Nanotubes, *Carbon*, 2002, **40**, 1741–1749.
- 41 C. Mercader, A. Lucas, A. Derre, C. Zakri, S. Moisan, M. Maugey and P. Poulin, Kinetics of Fiber Solidification, *Proc. Natl. Acad. Sci. U. S. A.*, 2010, **107**, 18331–18335.
- 42 G. Zhou, J. H. Byun, Y. Oh, B. M. Jung, H. J. Cha, D. G. Seong, M. K. Um, S. Hyun and T. W. Chou, Highly Sensitive Wearable Textile-Based Humidity Sensor Made of High-Strength, Single-Walled Carbon Nanotube/Poly(Vinyl Alcohol) Filaments, *ACS Appl. Mater. Interfaces*, 2017, **9**, 4788–4797.
- 43 A. Rubio, J. L. Corkill and M. L. Cohen, Theory of Graphitic Boron Nitride Nanotubes, *Phys. Rev. B: Condens. Matter Phys.*, 1993, **49**, 5081.
- 44 J. A. Fagan, M. Zheng, V. Rastogi, J. R. Simpson, C. Y. Khripin, C. A. Silvera Batista and A. R. Hight Walker, Analyzing Surfactant Structures on Length and Chirality Resolved (6,5) Single-Wall Carbon Nanotubes by Analytical Ultracentrifugation, *ACS Nano*, 2013, **7**, 3373–3387.



- 45 S. Lin and D. Blankschtein, Role of the Bile Salt Surfactant Sodium Cholate in Enhancing the Aqueous Dispersion Stability of Single-Walled Carbon Nanotubes: A Molecular Dynamics Simulation Study, *J. Phys. Chem. B*, 2010, **114**, 15616–15625.
- 46 M. Calvaresi, S. Hoefinger and F. Zerbetto, Probing the Structure of Lysozyme-Carbon-Nanotube Hybrids with Molecular Dynamics, *Chem.-Eur. J.*, 2012, **18**, 4308–4313.
- 47 V. Castelletto, E. P. G. Areas, J. A. G. Areas and A. F. Craievich, Effects of Tetramethylurea on the Tertiary Structure of Lysozyme in Water, *J. Chem. Phys.*, 1998, **109**, 6133–6139.
- 48 D. W. Horn, K. Tracy, C. J. Easley and V. A. Davis, Lysozyme Dispersed Single-Walled Carbon Nanotubes: Interaction and Activity, *J. Phys. Chem. C*, 2012, **116**, 10341–10348.
- 49 A. D. Smith McWilliams, Z. Tang, S. Ergülen, C. A. de Los Reyes, A. A. Martí and M. Pasquali, Real-Time Visualization and Dynamics of Boron Nitride Nanotubes Undergoing Brownian Motion, *J. Phys. Chem. B*, 2020, **124**, 4185–4192.
- 50 M. Subramanian, B. S. Sheshadri and M. P. Venkatappa, Interaction of Proteins with Detergents: Binding of Cationic Detergents with Lysozyme, *J. Biosci.*, 1986, **10**, 359–371.
- 51 L. W. Taylor, O. S. Dewey, R. J. Headrick, N. Komatsu, N. M. Peraca, G. Wehmeyer, J. Kono and M. Pasquali, Improved Properties, Increased Production, and the Path to Broad Adoption of Carbon Nanotube Fibers, *Carbon*, 2021, **171**, 689–694.
- 52 V. R. Kode, K. R. Hinkle and G. Ao, Interaction of DNA-Complexed Boron Nitride Nanotubes and Cosolvents Impacts Dispersion and Length Characteristics, *Langmuir*, 2021, **37**, 10934–10944.
- 53 Y.-J. You, J.-H. Kim, K.-T. Park, D.-W. Seo and T.-H. Lee, Modification of Rule of Mixtures for Tensile Strength Estimation of Circular GFRP Rebars, *Polymers*, 2017, **9**, 682.
- 54 R. J. Mora, J. J. Vilatela and A. H. Windle, Properties of Composites of Carbon Nanotube Fibres, *Compos. Sci. Technol.*, 2009, **69**, 1558–1563.
- 55 C. Lu, C. Blackwell, Q. Ren and E. Ford, Effect of the Coagulation Bath on the Structure and Mechanical Properties of Gel-Spun Lignin/Poly(Vinyl Alcohol) Fibers, *ACS Sustainable Chem. Eng.*, 2017, **5**, 2949–2959.
- 56 D. Lai, Y. Wei, L. Zou, Y. Xu and H. Lu, Wet Spinning of PVA Composite Fibers with a Large Fraction of Multi-Walled Carbon Nanotubes, *Prog. Nat. Sci.: Mater. Int.*, 2015, **25**, 445–452.

